Journal of Solid Mechanics Vol. 15, No. 2 (2023) pp. 174-184
DOI: 10.22034/jsm.2022.1953532.1734

Research Paper

A Study on Stiffness of a Defective Rippled Graphene Using Molecular Dynamics Simulation

A. Hamzei [1,*], E. Jomehzadeh [1], M.Rezaeizadeh [1], M. Mahmoodi [2]

[1]*Department of Mechanical Engineering, Graduate University of Advanced Technology, Kerman, Iran*
[2]*Department of Mechanical Engineering, Shahid Bahonar University, Kerman, Iran*

Received 25 February 2023; accepted 15 April 2023

ABSTRACT

Graphene without defects exhibits extraordinary mechanical properties, while defects such as vacancies and Stone-Wales usually impose a suffering effect on graphene's properties. On the other hand, strictly two-dimensional crystals are expected to be unstable due to the thermodynamic requirement for the existence of out-of-plane bending with interatomic interaction generating a mathematical paradox. This paper researches the fracture strength and the stretching stiffness of a rippled defective graphene that is placed under the loading pressure of uniaxial tensile. With the purpose of replicating a model for carbon atoms' covalence bonding, a molecular dynamics simulation is carried out. This is sorted according to the adaptive intermolecular reactive bond order potential function. The degree of the temperature of the system throughout the experiment is contained through the Nose-Hoover thermostat. The software package large-scale atomic/molecular massively parallel simulator is utilized for the aim of simulation the desired bond formation in the graphene layer structure. The present study offers a physical insight into the mechanisms of topological mechanical defects of graphene, and we propose static ripples as one of the key elements to accurately understand the thermo-mechanics of graphene. The results revealed that the fracture strength of a rippled graphene is significantly reduced when it contains defects, and fracture stress and strain with different vacancy defects are presented and compared.

Keywords: Rippled graphene; Molecular dynamics modeling; Defects; Mechanical properties; Temperature.

1 INTRODUCTION

GRAPHENE [1], can be describes as a single-layered honeycomb lattice. This structure composed of carbon atoms has garnered considerable interest following experimental results that proved its properties regarding complex low-dimensional electronic characteristics as well as its two-dimensional lattice stability. The high strength

*Corresponding author.
E-mail address: amin.hamzei@gmail.com (A.Hamzei)

of these nanostructures makes them appropriately promising for applications including Nano-composite materials [2,3]. Graphene could be created by chemical vapor deposition (CVD), mechanical exfoliation, chemical reduction of graphene sheets, etc. As it has been confirmed that the properties of graphene can be verified by chemical functionalization [4]. However, material production techniques and chemical remedy might introduce structural defects in graphene, like those of vacancies and Stone–Wales (S-W) types. Previous literature has provided evidence on defects that they include vacancies [5], dislocations [6], grain boundaries, and Stone-Wales [7,8] in graphene sheets [9-12] and nanotubes [13,14]. In order to successfully produce high-performance carbon materials, it is necessary to clarify the influence of defects on graphene and graphite's mechanical and electrical properties. In the experimental part, Lee et al. [15] outlined that the value of 1 ± 0.1 *TPa* was Young's modulus of graphene, while the following value and strain were related to the ultimate stress with the former being 130 ± 10 *GPa* and the latter being 0.25. Aljedani et al. [16] studied the behavior of a wrinkled graphene sheet supported on a metal substrate, resulting in their presentation of a variational model for a wrinkled graphene sheet. Parabhakar and Melnik [17] focused on sheets of graphene and graphene nanoribbons with specific analysis on the rippling effect on such sheets. Friedrich and Stefanelli [18] studied ripples in graphene, and they reported that almost minimizers of the configurational energy develop waves with a specific wavelength, independently of the sample size. Jiang et al. [19] undertook the research of various factors including sizes and isotopic disorders as well as distinct temperatures in Young's modulus of SLGs. Yousefi et al. [20] showed Thermal properties in the nanoporous graphene, containings a series of nanoporous in an ordered direction. They investigated the dependence of thermal conductivity on edge chirality, sample size, and porosity concentration. Xiang et al. [21] analyzed the buckling of the single-layered graphene under tension through MD simulations. Tensile characteristics of graphene and CNTs were carried out by Xiao et al. [22], these MD simulations included multiple S-W defects. Their results conferred that such nanomaterials have a high chance of losing their strength by a considerable amount if defects are detected in the structure. Kahara and Koskinen [23] published a review of later reports of laser-controlled creation of line defects in graphene sheets. They revealed how line defects can be utilized to control rippling in two-dimensional materials. Simulations showed that elastic sheets with networks of line defects produce ripple that induce considerable out-of-plane rigidification and in-plane softening with nonlinear elastic behavior. Rouhi [24] researched the molecular dynamics simulation of the graphdiyne nanotubes with specific focus on characteristics related to the mechanical aspect. In this case of having zigzag nanotubes carrying the same characteristics including geometrical parameters as the zigzag graphdiyne NTs, the aforementioned modulus was observed to the present in larger proportion in the latter type of nanotubes. Under an increasing thermal conditioning, consequential reduction was present in characteristics including ultimate stress, the stress of fracture initiation, as well as Young's modulus of the nanotubes. Moreover, through the analysis, it was understood that the expansion in defect percentage can lead to nonlinear degradation in the discussed Young's modulus of the graphdiyne NTs. Ghorbanpour Arani et al. [25] investigated nonlinear dynamic stability of simply supported graphene integrated with ZnO sensors and actuators based on viscoelastic surface and nonlocal piezoelasticity theories via refined Zigzag theory. Torabi rad and Froutan [26] investigated the wettability properties of Penta-Graphene and Graphene, ReaxFF predict experimental contact angle for the former was more hydrophobic than the latter. In addition, the wettability of net *C*, net *W*, and net *Y* was investigated by MD simulation, revealing that the tetrahedrality of water molecules at the interfaces of the three substrates was uniform. It was also observed that the hydrogen bonding exhibited nearly identical effects on all three substrates. However, the degree of droplet displacement varied, with the highest displacement observed on net *W* and the lowest on net *Y* [27]. Fang et al. [28] studied the buckling of graphene with a hole subjected to in-plane shear displacements at different temperatures by MD simulation. They appealed that a sudden drop of shear stress occurs due to wrinkling, and the shear stress is rose with increasing temperature. Ghorbanpour Arani et al. [29] studied on a smart single-layer graphene sheet (SLGS) is analytically modeled and its buckling is controlled using coupled polyvinylidene fluoride (PVDF) nanoplates and found that the effect of external voltage becomes more prominent at higher nonlocal parameter and shear modulus. Fasolino et al. [30] outlined the ripples can be detected in the suspended graphene within the 0.07 nm maximum deflection. Through MD simulation, Xiang and Shen [31] after analyzing rippled single-layered graphene sheets and their shear buckling in various thermal conditionings realized that the armchair graphene does not display as much shear buckling capacity as that of rectangular zigzag ones. Researchers observed ripples in suspended layers of graphene sheets [32], and it has been proposed that thermal fluctuations in the material could be the cause of the ripples. Since the exterior of the rippled graphene alters into a rough and dented surface, the fracture stress becomes conclusively lower despite its behavioral display of softened stretching. It is noteworthy to mention that the uniaxial tensile loading applied to a rippled graphene has shown to have a failure strain that is lower than that of the flat counterpart [33]. According to Shenoy et al. [34], the tensions at the edges can result in the formation of intrinsic ripples in freestanding graphene sheets such ripples can occur regardless of changes to the temperature. the tensions on the compressive edge of the both types of sheets

result in numerous formations of degenerated modes since they undergo out-of-plane warping. Ansari et al. [35] revealed that the presence of defects could considerably reduce the failure strain and the intrinsic strength of single-layered graphene sheets (SLGSs), while it has a slight effect on Young's modulus. Shen et al. [36] found that higher thermal conditioning will cause reduction in Young's modulus as opposed to the previous one, the shear modulus does not display as much reliance on thermal conditions. Furthermore, the difference between the zigzag and armchair sheets lied in the fact that the former was more susceptible to the influence of thickness. Chen et al. [37] reported that Young's modulus and fracture strength of polycrystalline graphene is more sensitive to the change in temperature and strain rate compared to the single-crystalline graphene. When temperature increases from 100 to 1200 K, the fracture strength of polycrystalline graphene is reduced by around 45%. To have a clear understanding of rippled graphene, one can imagine a crumpled paper and then opened it. Now we can see a sheet of paper with static wrinkles as shown in Fig. 1; stretching wrinkled paper requires less energy than when it is flat. The exterior of the sheets can display various shapes of ripples and wrinkles. Numerous factors contribute to the occurrence of such crumples in the graphene's exterior since the natural structure of the sheet will be altered as a result of the ripples, including its electronic structure in a way that the carrier puddles end up becoming polarized. Furthermore, a pseudo-magnetic field could be created in bilayers which would shift the previous exterior of the graphene. Factors contributing to the crumple formations include thermal vibrations, thermodynamically unstable, edge instabilities, thermal contraction, dislocations, defects, pre-strained substrate-relaxation, surface anchorage, and high solvent surface tension during transfer. However, it reduces some of the mechanical properties, referred in the following. Therefore, in addition to simulating perfect graphene, rippled and defective graphene must be analyzed for certain applications so that its cost-effectiveness in having these models with lower mechanical properties can be determined.

In this paper, the effects of defects on the stretching stiffness of a rippled graphene are investigated by Molecular Dynamics simulation. Various frequencies are employed in order to replicate the rough and indented exterior of the graphene randomly. The initial locations of atoms are defined based on the rippling and defects, SV (single vacancy), DV (double vacancy), sextuple, and SW (Stone–Wales) of the graphene sheet. Then, the MD simulation with AIREBO potential function is used to obtain the stretching behavior of the suspended defective rippled graphene.

Fig.1
Crumpled paper will be much easier to stretch than when it is plane i.e. low elastic modulus.

2 GEOMETRICAL MODEL

Surface topography description is important in structures including contact, friction, lubrication, and wear. The same concept of roughness has statistical implications as it considers a number of factors, including sampling size and interval. Also, the uneven surface of a structure can result in a change in its specific stiffness (stiffness per mass density) hence, causing change in its mechanical behaviors. High specific stiffness of materials receives wide application in sensitive equipment, especially in Nano-scale systems where minimum structural weight is essential. Since the specific stiffness of graphene can be increased by opening crumpled graphene, some rippling is created on the surface of graphene in order to increase of its stiffness quality.

A variety of frequencies are applied in order to achieve the indented exterior of the rippled graphene along with a function selected randomly. The amount of 0.5 °A is chosen for the ripple's maximum amplitude. Fig. 2 represents the information.

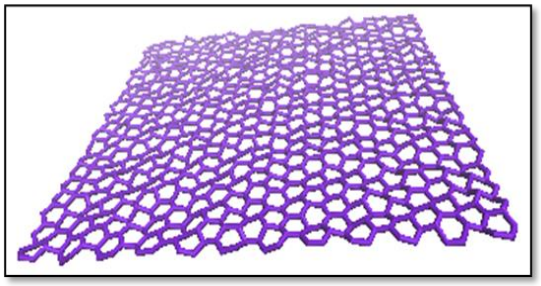

Fig.2
The geometry of a rippled grapheme.

It is also possible that graphene has a defect in its structure as it has been demonstrated that carbon structures such as nanotubes and graphene are rarely perfect, and their defect density is not zero, even in highly pure crystalline systems. Defects play a significant effect on the physical properties of a graphene. Here, four types of defects, as shown in Fig. 3. are modeled, and their effects on stretching stiffness and graphene strength are examined.

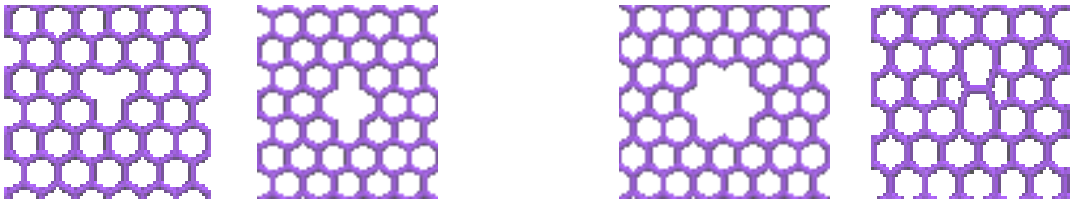

(a) (b) (c) (d)

Fig.3
Different types of defects in grapheme a) Single vacancy b) Double vacancy c) Sextuple d) Stone-Wales.

3 MODELING AND SIMULATION

The simulated model of graphene is built up with 1500 atoms with geometrical dimensions of 6 *nm* × 6 *nm*, as shown in Fig. 4. In the MD simulation enforced in package LAMMPS [38], the interaction between carbon atoms is represented by the adaptive intermolecular reactive bond order (AIREBO) potential, that might accurately capture the interactions between carbon atoms as well as bond breaking and re-forming with periodic boundary conditions (PBC) within the in-plane two directions. In Eq. (1) you can find three potential components of AIREBO [39]:

$$E^{AIREBO} = \frac{1}{2}\sum_i \sum_{i \neq j} \left[E_{ij}^{REBO} + E_{ij}^{LJ} + \sum_{K \neq i,j} \sum_{L \neq i,j,k} E_{ijkl}^{Torsion} \right] \tag{1}$$

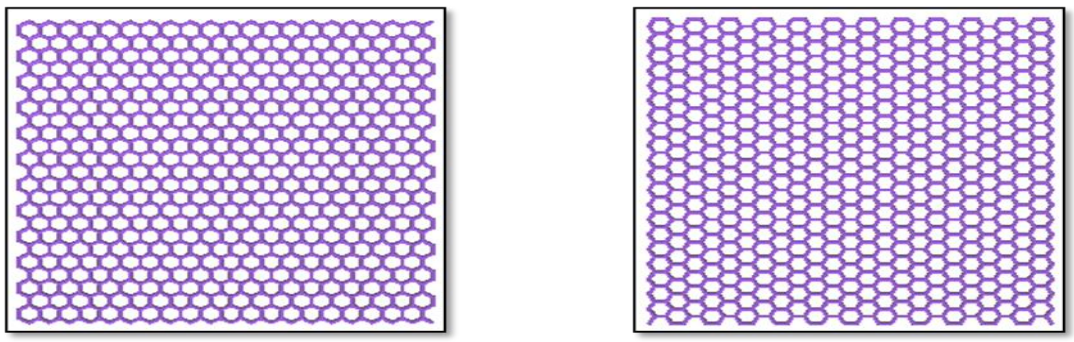

(a) (b)

Fig.4
The geometric of a) Zigzag b) Armchair grapheme.

where E_{ij}^{REBO} is the REBO part, which explains the bonded interaction between atoms based on the second-generation reactive empirical bond order potentials of Brenner, E_{ij}^{LJ} is the Lennard-Jones potential that considers those types of atom interactions that belong to the category of nonbonded; torsional atom interactions and total energy based on the dihedral system angles are represented by $E_{ijkl}^{Torsion}$. The default value of cut-off distance for the non-bond interaction was $1.75°A$. In this equation, the short-range of C–C atoms interaction are described by the term E_{ij}^{REBO} (with distance $r < 2.0\ °A$) and longer range by E_{ij}^{LJ} ($2.0\ °A < r <$ cut-off distance). In fact, the main advantage of AIREBO potential is the consideration of nonbonded interactions in the systems where they play a key role in non-flat structures such as rippled graphene.

The tensile load is applied to the graphene along both directions of armchair and zigzag. The thermal conditioning of $T = 300\ K$ which is equivalent to the room temperature is the condition under which simulation are applied in the conical ensemble. To avoid the thermal effect and to maintain constant temperature the structures were permitted to relax at zero pressure using constant pressure-temperature (i.e., NPT ensemble). The Nose-Hoover thermostat is selected to ensure the stability of the thermal condition in the system for the duration of the experiment. Moreover, the Velocity-Verlet integration algorithm is used to solve the equations of motion through time with a time step of $dt = 1\ fs$. The strain rate at which the simulation was conducted was at 0.001 ps-1.

Out of the possible defect types that potentially happen in nanostructures two types are more likely including that of vacancies and Stone-Wales. The latter is topological and happens when the carbon bond is found to be rotated about 90 degrees. Firstly, the structure of graphene sheets was prepared, then energy minimization was done to achieve the thermally stable morphology and configuration of minimum potential energy which was further used in MD simulation. To equilibrate and relax the structure of graphene, constant temperature and pressure isothermal-isobaric ensemble (NPT ensemble) was used subsequently. The structure was relaxed for 100,000 steps so that the inner stress of the graphene sheet can be eliminated. This procedure should be done before applying an external load. The analytical graphene models with cluster-type vacancies are shown in Fig. 3. Also, the uneven surface of the rippled graphene might include wrinkles which have occurred randomly each resulting from a variety of amplitudes and frequencies. Fig. 2 illustrates such sheets that are also considered to be open crumpled graphene. To perceive a comparison, two more graphene sheets with an equivalent geometrical size were simulated as well, one of which was perfect, and the other contained one of the defects.

4 RESULT AND DISCUSSION

The potential energy of the graphene sheet is an important result and output in the molecular dynamics simulation. The changes of potential energy with time are shown in Fig. 5. The system's potential energy is approximately constant during the relaxation period, though it begins to increase once strain is applied.

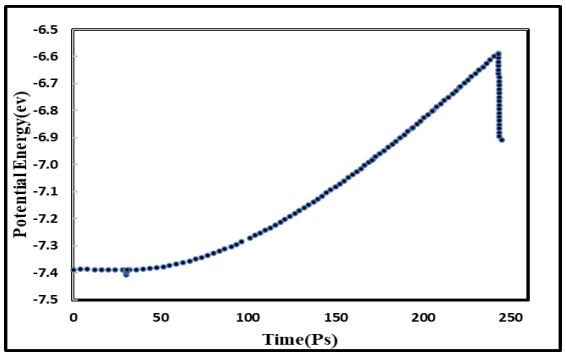

Fig.5
Potential energy changes with time in graphene.

The ripple pattern in graphene may be affected by various factors, including temperature and the size of the graphene sheet. As an instance, when the thermal conditioning is near absolute zero ripples do not appear on the suspended graphene, though as the thermal conditioning increases ripples become visible. In order to confirm the numerical aspect of the experiment, first, a graphene sheet was studied in its perfect conditioning and the relevant fracture length was calculated and examined. In Fig. 6, the nominal results in the literature are presented as a measure against the strain-stress curve at 300 K which had tension load applied in zigzag direction. It can be seen

that the present result provides desirable accuracy as compared to Zhao et al. [40] reviewed model in which the graphene was at thermal conditioning equivalent to that of a room. In this model a MD simulation of 3936 atoms (100.8 $°A \times 102.2\ °A$) were carried out for the NPT ensemble. The model was also equipped with periodic boundary conditions (PBC) in the in-plane two directions.

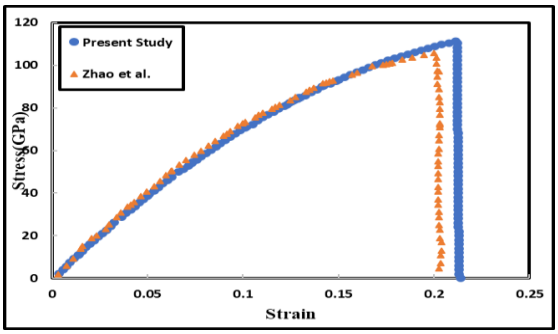

Fig.6
Comparison of the stress-strain curve of flat and perfect graphene with Zhao et al. [40].

The administered tension and stress onto the compositions and materials until a breaking point is achieved is defined as the fracture strength. Both of the graphene sheets categorized as zigzag and armchair according to Zhao et al.'s research is reported to be 107 *GPa* for the former category and the 90 *GPa* for the latter and in this paper the fracture strength is 110 *GPa* and 92 *GPa*. Furthermore, the previous literature's results are available for measuring against the Young's modulus of flat graphene. Table 1. displays this information that were entirely performed under the same thermal conditioning of 300 *K*, and the difference in Young's modulus values could be influenced by factors such as the equilibrium, the dimensions of the graphene sheet, the type of potential chosen for the simulation, and how the system is minimized.

Table 1
A comparison of the computed Young's modulus of a perfect grapheme.

References	Method	Young's Modulus (*GPa*)
Present model	MD	834
Ansari et al.[35]	MD	800
Pei et al. [4]	MD	830
Setoodeh et al. [5]	MD	922
Li et al. [6]	MD	911
Lee et al. [15]	Experimental	1000

The strain-stress curve of rippled graphene with random wrinkles of $0.3°A$ amplitudes under uniaxial tensile load in the temperature range of 1 *K* to 1000 *K* is shown in Fig. 7. While the increase in temperature, stress drops. Fig. 8. presents the rippled graphene strain-stress curve in order to provide a clear comparison of zigzag and armchair edges, Young's modulus, also, displays a similar behavior to that of a perfect graphene sheet as the decrease in stress is resulted from temperature increase.

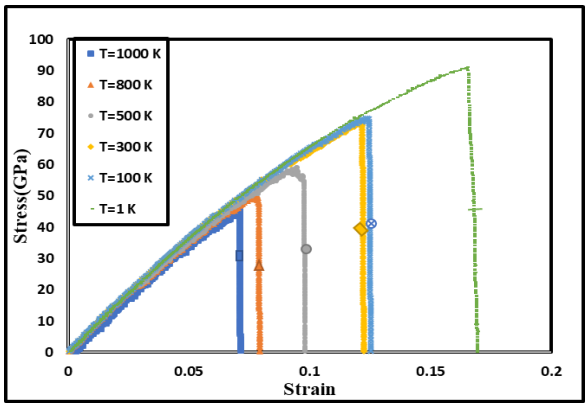

Fig.7
Stress-strain curves of rippled graphene at different temperature.

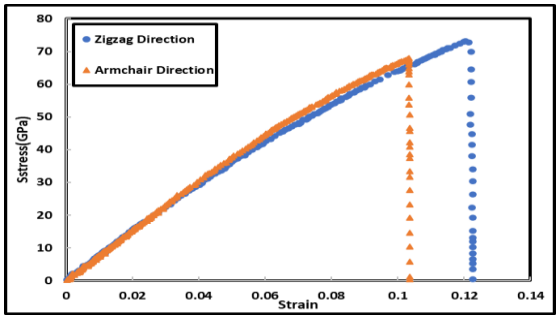

Fig.8
Stress-strain curves of rippled graphene at 300 *K*.

It can be seen that the rippled graphene has a softening stretching behavior. As flat graphene is converted to an uneven surface, its fracture stress and strain will be reduced. As an instance, the decrease rate in the zigzag graphene for the characteristic of fracture stress is about 3.64%, while the strain characteristic is around 4.72%. These amounts show to be different for the other type of graphene sheet with the first characteristic being 7.61% and the second one 7.95%, these values are illustrated in Table 2. The values of stress and strain showed significant decrease compared to those of the perfect flat graphene. It may be seen that the strain and fracture stress of the defective rippled graphene in zigzag direction are higher than those of the armchair. Therefore, it can be concluded that the zigzag rippled graphene displays more strength compared to the armchair one. As shown in the table, existing ripples in graphene, such as crumpled paper, reduces the fracture stress and strain, so that the fracture stress from 110 and 92 *GPa* at the zigzag and armchair edges has reached 106 and 85, respectively. If rippled graphene has a defect, it is clear that the values of fracture stress and strain will be significantly reduced compared to smooth graphene sheets. For example, it can be seen that rippled graphene has a fracture stress of 96 and a strain of 9.6 in the graphene with Stone-Wales defect, which has decreased by 12.73% and 54.72% compared to flat graphene without defect.

Table 2
Comparison fracture stress and strain between perfect and defective graphene with 0.3A amplitudes.

		Flat graphene	Rippled graphene	Ripples graphene with SV	Ripples graphene with DV	Ripples graphene with SW
Zigzag direction	Fracture stress	110 *GPa*	106 *GPa* (-3.64%)	80 *GPa* (-27.28%)	80 *GPa* (-27.28%)	96 *GPa* (-12.73%)
	Strain	21.2	20.2 (-4.72%)	13.1 (-38.21%)	12.9 (-39.15%)	9.6 (-54.72%)
Armchair direction	Fracture stress	92 *GPa*	85 *GPa* (-7.61%)	76 *GPa* (-17.4%)	76 *GPa* (-17.4%)	67 *GPa* (-27.17%)
	Strain	15.1	13.9 (-7.95%)	12 (-20.53%)	12.2 (-19.21%)	9.2 (-39.07%)

The Young's modulus on the armchair direction showed be less than that of the zigzag direction, whereas the fracture strength and strain were larger than the latter group indicating a typical anisotropic behavior. The fracture process of graphene sheets with defects is shown in Figs. 9-12. The open-source visualization tools of VMD are used to present the atomic configurations [41].

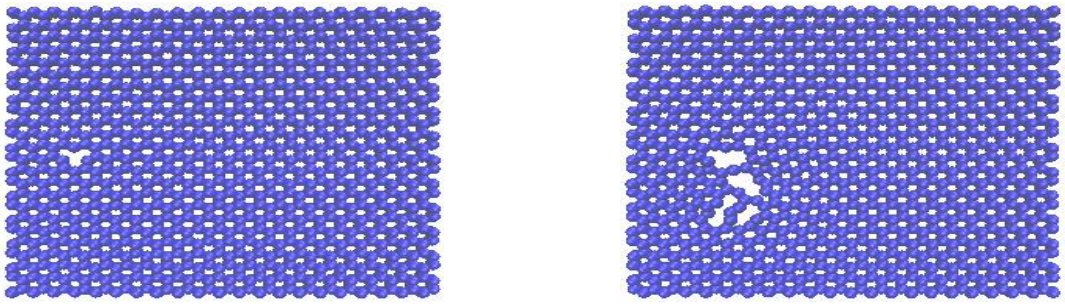

Fig.9
The fracture process in graphene sheet with a single vacancy.

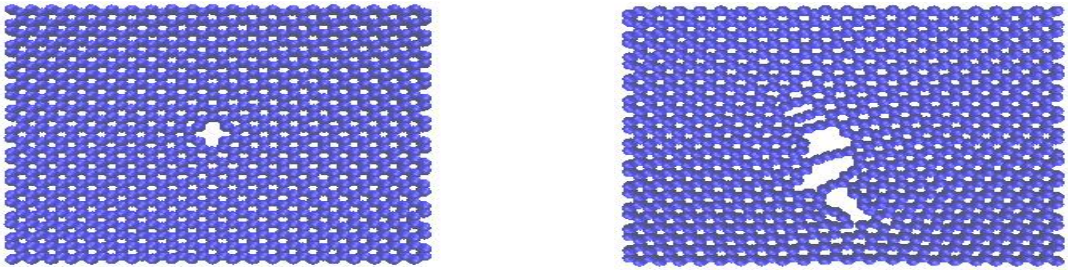

Fig.10
The fracture process in graphene sheet with double vacancy.

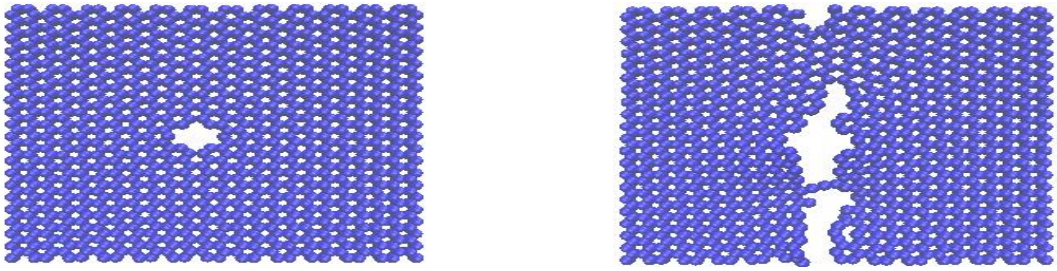

Fig.11
The fracture process in graphene sheet with sextuple.

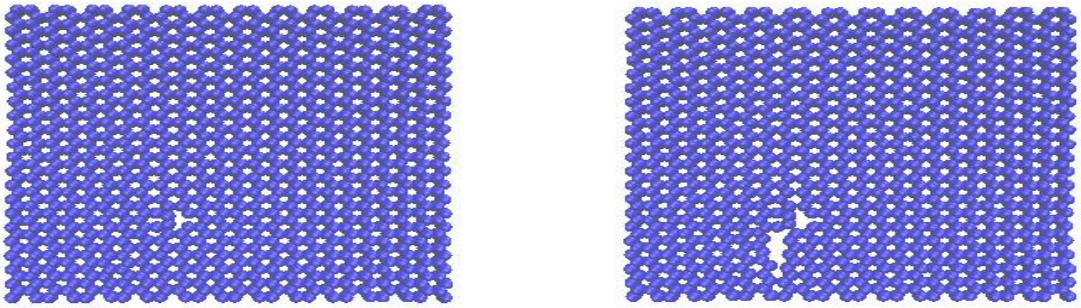

Fig.12
The fracture process in graphene sheet with Stone-Wales.

As shown in Fig. 13. in the Stress-Strain curve in flat graphene, the double vacancy and sextuple defects sustain lower stress and strain in comparison with other defects in the zigzag direction. Furthermore, the sextuple and Stone-Wales defects display less mechanical properties in the armchair direction.

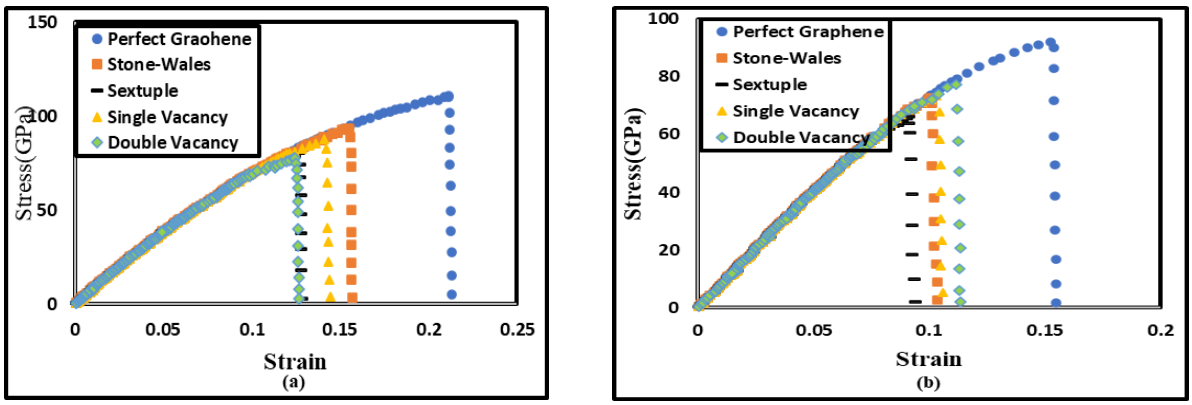

Fig.13
Stress-strain curves of defective flat graphene for different defects a) Zigzag b) Armchair.

Fig. 14. presents all the information regarding analyzed defects in the rippled graphene of zigzag and armchair directions. As shown in the zigzag graphene Stress-Strain curve, Stone-Wales defect bears more strain than other defects, and in armchair direction, sextuple vacancy defect and Stone-Wales defect have less stress and strain than the rest.

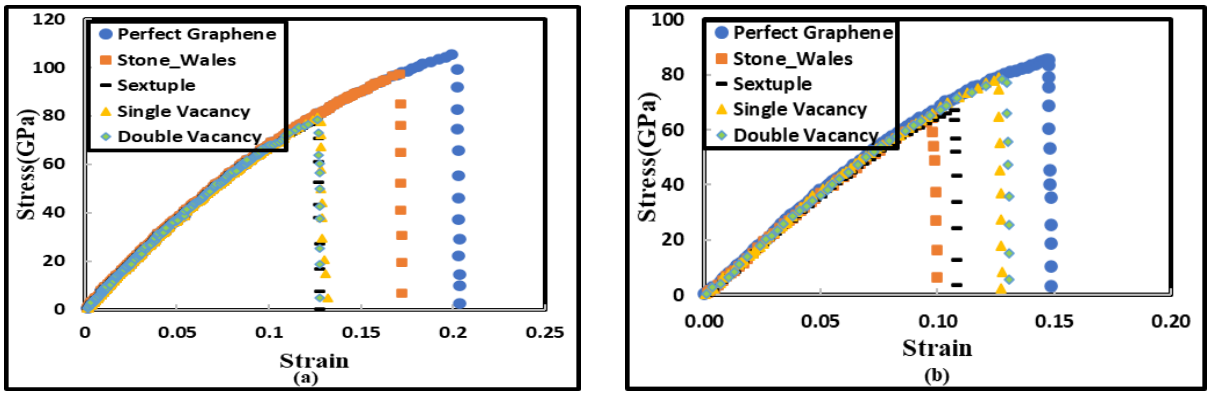

Fig.14
Stress-strain curves of defective rippled graphene with 0.3 °*A* amplitude for different defects: a) Zigzag b) Armchair.

The other model, Fig.15., includes a rough and dented exterior for the rippled graphene and the design is replicated through the specified trigonometric sine form and unit frequency of 0.5 °*A* amplitude.

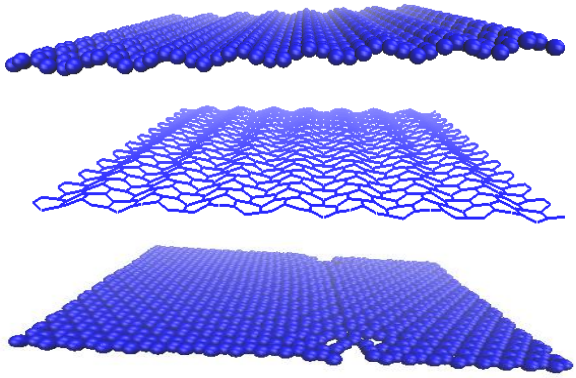

Fig.15
Display of rippled graphene sheet from the beginning of tensile simulation until failure.

Fig.16. Shows all of the investigated defects in Sine shape rippled graphene in both the armchair and zigzag directions. As it is known, the Stress-Strain curve of zigzag graphene with vacancy defects bears more strain than other ones.

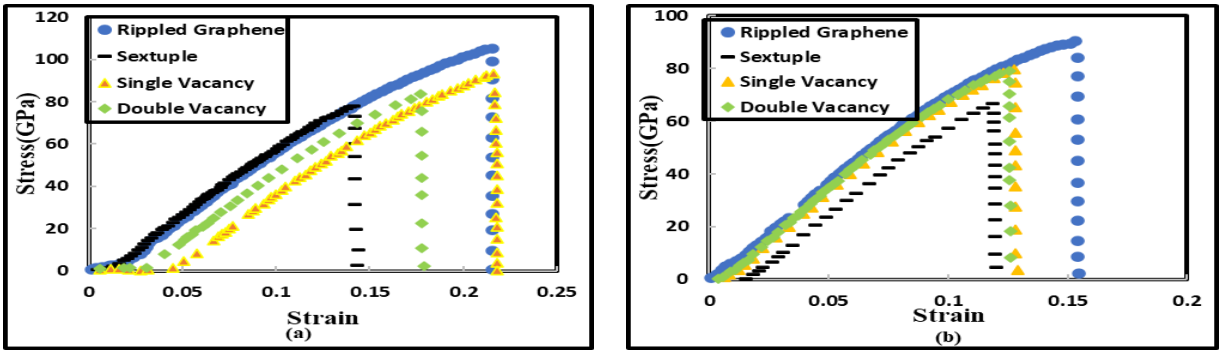

Fig.16
Stress-strain curve of defective rippled graphene with 0.5 °A amplitude for different defects: a) Zigzag b) Armchair.

A comparison of the stress-strain curve between the edges of the armchair and zigzag is shown in Fig. 17. It seems that, as in previous cases, the fracture stress in the armchair direction is lower than the value in the zigzag direction.

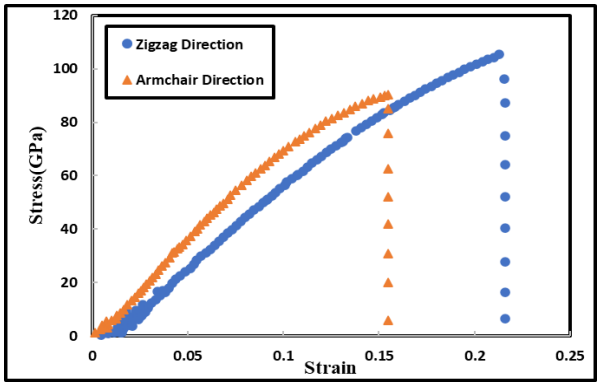

Fig.17
Stress-strain curve of rippled graphene by the trigonometric sine shapes.

5 CONCLUSION

In this article, molecular dynamics simulation in rippled graphene without defect was developed to be researched based on the AIREBO potential function at the different temperature as shown in Fig. 7. Moreover, for defective rippled graphene this method was studied at constant room temperature of $T = 300K$. The Nose-Hoover thermostat was utilized to maintain the temperature of the system when analyzing the fracture strength of the defective rippled graphene. Conclusively, the rippled graphene and defective rippled graphene have softening stretching behavior. Also, the fracture stress of graphene is reduced as its surface becomes uneven and imperfect.

REFERENCES

[1] Novoselov K.S., Geim A.K., Morozov S.V., Jiang D., 2004, *Electric Field Effect in Atomically Thin Carbon Films*, Science Magazine.

[2] Babaei M., Kiarasi F., Tehrani M.S., Hamzei A., Mohtarami E., Asemi K., 2022, Three dimensional free vibration analysis of functionally graded graphene reinforced composite laminated cylindrical panel, *Proceedings of The Institution of Mechanical Engineers, Part L, Journal of Materials: Design and Applications* **236**(8):1501-1514.

[3] Nouroozi Masir A., Darvizeh A., Zajkani A., 2019, Temperature effect on mechanical properties of top neck mollusk shells nano-composite by molecular dynamics simulations and nano-indentation experiments, *Journal of Solid Mechanics* **11**(4): 902-917.

[4] Pei Q.X., Zhang Y.W., Shenoy V.B., 2010, A molecular dynamics study of the mechanical properties of hydrogen functionalized graphene, *Carbon* **48**: 898-904.

[5] Setoodeh A.R., Badjian H., Jahromi H.S., 2017, Atomistic study of mono/multi-atomic vacancy defects on the mechanical characterization of boron-doped graphene sheets, *Journal of Molecular Modeling* **23**: 2.

[6] Li M., Deng T., Zheng B., 2019, Effect of defects on the mechanical and thermal properties of graphene, *Nanomaterials* **9**: 347.

[7] Podlivaev A.I., Grishakov K.S., Katin, K.P., Maslov M.M., 2021, Stone–Wales bilayer graphene: structure, stability, and interlayer heat transfer, *JETP Letters* **114**: 143-149.

[8] Pozrikidis C., 2009, Effect of the Stone–Wales defect on the structure and mechanical properties of single-wall carbon nanotubes in axial stretch and twist, *Archive of Applied Mechanics* **79**: 113-123.

[9] Ghorbanpour Arani A., Jalaei M.H., 2016, Transient behavior of an orthotropic graphene sheet resting on orthotropic visco-Pasternak foundation, *International Journal of Engineering Science* **103**: 97-113.

[10] Zheng B., Gu G.X., 2020, Machine learning-based detection of graphene defects with atomic precision, *Nano-Micro Letters* **12**: 181.

[11] Shirzadi Jahromi H., Mehdipour F., Firoozi G., 2021, Fracture analysis of vacancy defected nitrogen doped graphene sheets via MD simulations, *Mapta Journal of Mechanical and Industrial Engineering* **5**(1): 18-23.

[12] Bedi D., Sharma S., Tiwari S.K., 2022, Effect of chirality and defects on tensile behavior of carbon nanotubes and graphene: Insights from molecular dynamics, *Diamond and Related Materials* **121**: 108769.

[13] Shariati A., Golkarian A., Jabbarzadeh M., 2014, Investigation of vibrational behavior of perfect and defective carbon nanotubes using non–linear mass–spring model, *Journal of Solid Mechanics* **6**(3): 255-264.
[14] Shi X., He X., Sun L., Liu X., 2022, Influence of defect number, distribution continuity and orientation on tensile strengths of the CNT-based networks: A molecular dynamics study, *Nanoscale Research Letters* **17**: 15.
[15] Lee C., Wei X., Kysar J.W., 2008, Measurement of the elastic properties and intrinsic strength of monolayer graphene, *Science* **321**: 385-388.
[16] Aljedani J., Chen M.J., Cox B.J., 2020, Variational model for a rippled graphene sheet, *RSC Advances* **10**: 16016.
[17] Prabhakar S., Melnik R., 2016, Ripples in graphene sheets and nanoribbons, *AST* **100**: 87-92.
[18] Friedrich M., Stefanelli U., 2020, Ripples in graphene: A variational approach, *Communications in Mathematical Physics* **379**: 915-954.
[19] Jiang J.W., Wang J.S., Li B., 2009, Young's modulus of graphene: a molecular dynamics study, *Physical Review B* **80**: 113405.
[20] Yousefi F., Khoeini F., Rajabpour A., 2020, Thermal conductivity and thermal rectification of nanoporous graphene: A molecular dynamics simulation, *International Journal of Heat and Mass Transfer* **146**: 118884.
[21] Xiang Y., Shen H., 2015, Shear buckling of rippled graphene by molecular dynamics simulation, *Materials Today Communications* **3**: 149-155.
[22] Xiao J.R., Staniszewski J., Gillespie J.W., 2010, Tensile behaviors of graphene sheets and carbon nanotubes with multiple StoneWales defects, *Materials Science and Engineering* **527**: 715-723.
[23] Kahara T., Koskinen P., 2020, Rippling of two-dimensional materials by line defects, *Physical Review B* **102**: 075433.
[24] Rouhi S., 2019, On the mechanical properties of the graphdiyne nanotubes: a molecular dynamics investigation, *Brazilian Journal of Physics* **49**: 654-666.
[25] Ghorbanpour Arani A., Kolahchi R., Zarei M., 2015, Visco-surface-nonlocal piezoelasticity effects on nonlinear dynamic stability of graphene sheets integrated with ZnO sensors and actuators using refined zigzag theory, *Composite Structures* **132**: 506-526.
[26] Torabi Rad M., Foroutan M., 2022, Wettability of penta-graphene: A molecular dynamics simulation approach, *The Journal of Physical Chemistry C* **126** (3): 1590-1599.
[27] Hamzei A., Hajiabadi H., Rad M.T., 2023, Wettability of net C, net W and net Y: a molecular dynamics simulation study, *RSC Advances* **13**(4): 2318-2328.
[28] Fang T.H., Chang W.J., Lin K.P., Shen S.T., 2014, Stability and wrinkling of defective graphene sheets under shear deformation, *Current Applied Physics* **14**(4): 533-537.
[29] Ghorbanpour Arani A., Ebrahimi F., 2015, *Modeling and Control of a Smart Single-Layer Graphene Sheet*, Graphene - New Trends and Developments.
[30] Fasolino A., Los J.H., Katsnelson M.I., 2007, Intrinsic ripples in graphene, *Nature Materials* **6**: 858-861.
[31] Xiang Y., Shen H., 2015, Shear buckling of rippled graphene by molecular dynamics simulation, *Materials Today Communications* **3**: 149-155.
[32] Blees M.K., Barnard A.W., Rose P.A., Roberts S.P., McGill K.L., Huang P.Y., Ruyack A.R., Kevek J.W., Kobrin B., Muller D.A., McEuen P.L., 2015, Graphene kirigami, *Nature* **524**(7564): 204-207.
[33] Hamzei A., Jomehzadeh E., Rezaeizadeh M., 2019, Softening effect in stretching stiffness of a rippled graphene: molecular dynamics simulation, *Journal of Mechanical Engineering* **3**(1): 89-94.
[34] Shenoy V.B., Reddy C.D., Ramasubramania A., Zhang Y.W., 2008, Edge-stress-induced warping of graphene sheets and nanoribbons, *Physical Review Letters* **101**: 245501.
[35] Ansari R., Ajori S., Motevall B., 2012, Mechanical properties of defective single-layered graphene sheets via molecular dynamics simulation, *Superlattices Microstruct* **51**(2): 274-289.
[36] Shen L., Shen H.S., Zhang C.L., 2010, Temperature-dependent elastic properties of single-layer graphene sheets, *Materials and Design* **31**: 4445-4449.
[37] Chen M.Q., Quek S.S., Sha Z.D., Chiu C.H., Pei Q.X., Zhang Y.W., 2015, Effects of grain size, temperature and strain rate on the mechanical properties of polycrystalline graphene, a molecular dynamics study, *Carbon* **85**: 135-146.
[38] Plimpton S., 1995, Fast parallel algorithms for short-range molecular dynamics, *Journal of Computational Physics* **117**(1): 1-19.
[39] Stuart S.J., 2000, A reactive potential for hydrocarbons with intermolecular interactions, *Journal of Chemical Physics* **112**: 6472-6486.
[40] Zhao H., Min K., Aluru N.R., 2009, Size and chirality dependent elastic properties of graphene nanoribbons under uniaxial tension, *Nano Letters* **9**(8): 3012-3015.
[41] Humphrey W., Dalke A., Schulten K., 1996, Vmd: Visual molecular dynamics, *The Journal of Molecular Graphics* **14**: 33-38.